


Tunneling into a Finite Luttinger Liquid Coupled to Noisy Capacitive Leads

Antonio Štrkalj, Michael S. Ferguson, Tobias M. R. Wolf, Ivan Levkivskiy, and Oded Zilberberg
Institute for Theoretical Physics, ETH Zurich, 8093 Zurich, Switzerland

 (Received 18 September 2018; revised manuscript received 11 January 2019; published 29 March 2019)

Tunneling spectroscopy of one-dimensional interacting wires can be profoundly sensitive to the boundary conditions of the wire. Here, we analyze the tunneling spectroscopy of a wire coupled to capacitive metallic leads. Strikingly, with increasing many-body interactions in the wire, the impact of the boundary noise becomes more prominent. This interplay allows for a smooth crossover from standard 1D tunneling signatures into a regime where the tunneling is dominated by the fluctuations at the leads. This regime is characterized by an elevated zero-bias tunneling alongside a universal power-law decay at high energies. Furthermore, local tunneling measurements in this regime show a unique spatial dependence that marks the formation of plasmonic standing waves in the wire. Our result offers a tunable method by which to control the boundary effects and measure the interaction strength (Luttinger parameter) within the wire.

DOI: [10.1103/PhysRevLett.122.126802](https://doi.org/10.1103/PhysRevLett.122.126802)

Advances in control and design of mesoscopic systems have made it possible to realize a variety of ultrasmall electronic tunnel junctions [1,2]. In such junctions, many-body interactions and coherent effects compete with the charge fluctuations and impedance of the environment to profoundly impact the resulting tunneling characteristics; the tunneling inside the junction excites the electromagnetic modes of an external circuit making it extremely sensitive to the circuit's impedance [1–5]. This competition alters the tunneling density of states (TDOS) of the various device constituents, with a wide variety of such effects seen in, e.g., normal-metal tunnel junctions [6], Josephson junctions [7], and transmission lines [8]. Particular examples of such effects include, among others, the Coulomb blockade [9], the Kondo effect [10–12], and Andreev bound modes [13–16].

Tunnel junctions involving one-dimensional (1D) quantum wires are especially intriguing, since many-body interactions fundamentally alter the emergent many-body physics compared with conventional Fermi-liquid metals. Interacting wires are better described using Tomonaga-Luttinger liquid (TLL) theory [17–19]: the low-energy elementary excitations in 1D appear as collective bosonic plasmon modes—in stark contrast to the constitutive fermionic electrons. Consequently, 1D systems show exotic phenomena, such as charge fractionalization of injected electrons [20,21], spin-charge separation [22,23], and zero-bias anomalies (ZBA) [24–27], all of which uniquely interplay with disorder [28,29], quasidisorder [30], and dissipation [31,32]. Such 1D effects are ubiquitous and have been observed in a wide variety of systems from nanotubes [33–36] to cleaved and V-groove GaAs wires [22,23,37,38] through quantum Hall edges [39–41] and engineered systems such as arrays of Josephson junctions [42,43], ultracold atoms in 1D optical superlattices [44,45],

spin chains [46], and 1D crystals made of gold atoms [47] or $\text{Li}_{0.9}\text{Mo}_6\text{O}_{17}$ [48–50].

Recently, significant progress was made in the description of realistic finite-sized 1D wires with boundary conditions both in and out of equilibrium [27,51–54]. These can generally be grouped into wires (i) with open boundaries [55–57], (ii) connected to Ohmic contacts [58], or (iii) coupled to inherently out-of-equilibrium charge distributions [27,53]. The coupling between the wire and the leads is usually treated as adiabatic on the scale of the Fermi wavelength. This suppresses backscattering and thus implies that dc transport through the wire cannot detect interaction effects [51,57,59–63]. In contrast, a tunnel junction, e.g., between a scanning tunneling microscope (STM) and the wire, is ideally suited to sense these effects, since it gives access to the wire's energy distribution function [64,65] or to the (local) TDOS [66] of the wire, respectively. The latter commonly displays power-law scaling dependent on the extent of many-body interactions in the system [51,67]—quantified by the Luttinger parameter K —and is strongly impacted by the boundaries, i.e., impedance of the environment [3,4].

In this work, we study the impact of noisy capacitive metallic leads adiabatically coupled to an interacting quantum wire on tunneling from an STM into the wire. The capacitance in the leads imposes a finite response time in the wire, suppressing its fast high-energy excitations. Surprisingly, with increasing many-body interactions, the impact of the boundary noise on the wire is enhanced. The TDOS then enters a regime where it is dominated by the classical impedance of the capacitive reservoirs: (i) at low energies, the finite length of the wire cuts off the expected 1D tunneling zero-bias anomaly [57,67], and a zero-bias tunneling peak appears instead as a function of the environment capacitance; (ii) at high energies, the characteristic power-law growth is replaced by a universal

ω^{-3} decay [3]. Interestingly, this interaction-noise competition introduces a unique spatial dependence to the TDOS, thus offering an external handle by which to control the correlations in the wire, such that its Luttinger parameter can be tunably detected. To emphasize these novel effects, we concentrate on a spinless model adiabatically connected to the leads. For a discussion of the effects of spin and tunnel coupling to leads we refer the reader to Refs. [55,68–70] and [71], respectively. In the interest of readability, we briefly introduce the system and state our main result before showing the technical steps required to obtain it.

We consider a finite 1D wire coupled to metallic leads, depicted as an outer circuit that is characterized by an Ohmic resistance R and the capacitance C , and probed by a nearby STM, see Fig. 1(a). The STM signal measures the local TDOS at position x along the wire [72],

$$\nu(x, \omega) = i \int dt e^{i\omega t} [G^>(x, t) - G^<(x, t)], \quad (1)$$

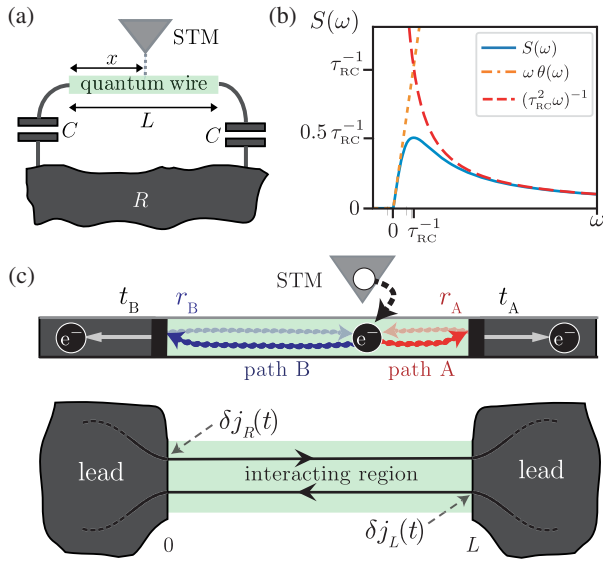


FIG. 1. (a) A 1D metallic quantum wire of length L is connected to metallic leads, depicted as an outer circuit that is characterized by an Ohmic resistance R and the capacitance to the ground C . The leads act as electron reservoirs with well-defined Fermi-Dirac distributions. The tunneling density of states [Eq. (1)] at position x along the wire is probed by a nearby scanning tunneling microscope (STM). (b) The zero temperature power spectral-density $S(\omega)$ of the RC-circuit’s noise [Eq. (3)] (blue solid line) and two asymptotic limits: (i) $\omega\tau_{RC} \ll 1$ (orange dot-dashed line) corresponding to the behavior of ideal Ohmic leads [73] and (ii) $\omega\tau_{RC} \gg 1$ (red dashed line) where high-energy fluctuations are damped by the circuit’s capacitance. (c) (Top) An electron from the STM induces 1D plasmonic excitations, for which the finite wire acts as an effective Fabry-Pérot interferometer with reflection (transmission) coefficients $r_{A,B}$ ($t_{A,B}$). (Bottom) A schematic view of the wire as left- and right-propagating modes connected to two identical leads, that impart current fluctuations $\delta j_{L/R}(t)$ onto the wire [Eq. (3)].

where ω is the electron’s energy, and $G^<(x, t)$ and $G^>(x, t)$ are the lesser and greater Green’s functions, respectively. We work in natural units, where $\hbar, e = 1$. In equilibrium, $G^<(x, t) = -G^>(x, -t)$ [72] and it suffices to analyze $G^<(x, t) = i\langle\psi^\dagger(x, t)\psi(x, 0)\rangle$, where we wrote its definition using the electronic field operator $\psi(x, t)$, and the average is taken with respect to the equilibrium ground state.

In one dimension, interacting electrons form a TLL with collective wavelike plasmonic excitations [17–19,51,74]. An electron injected from the STM into the wire excites plasmonic modes that propagate away such that the probability amplitude for the excitation to tunnel back into the STM decreases faster than in a noninteracting system. This decay manifests as a power law in the Green’s function [52,54,74]

$$\lim_{L \rightarrow \infty} G^<(x, t) = \frac{i\Lambda}{2\pi v_F} \frac{1}{(1 + i\Lambda t)^\alpha}, \quad (2)$$

where L is the length of the wire, Λ is the bandwidth of the electronic system, v_F is the Fermi velocity, and $\alpha = (K + K^{-1})/2 \geq 1$ is the interaction-dependent power-law exponent for the Luttinger parameter K . For noninteracting systems $K = 1$, and therefore $\alpha = 1$.

In a finite wire, the effects of many-body interactions compete with the noise arising at the boundaries [27,52,53,58]. The latter is characterized, in our case, by a power spectral density [75–77]

$$S(\omega) \equiv \langle\delta j_{L/R}(\omega)\delta j_{L/R}(-\omega)\rangle = \frac{\omega[1 - f_{FD}(\omega)]}{1 + \tau_{RC}^2\omega^2}, \quad (3)$$

where $\tau_{RC} = RC$ is the charging time of the capacitor in the outer circuit, and $f_{FD}(\omega) = (1 + \exp[\omega/k_B T])^{-1}$ is the Fermi-Dirac distribution in the left and right leads—assumed here to be identical and uncorrelated. The main difference between Eq. (3) and the power spectral density of ideal Ohmic leads is that the RC circuit acts as an additional low-pass filter [52,73], see Fig. 1(b).

We are interested in how the boundary noise (3) and interaction-induced 1D plasmons manifest in the electronic correlations in the wire, e.g., in $G^<(x, t)$. While the noise is characterized by the charging time τ_{RC} , we shall see below that the plasmonic waves are characterized by their time-of-flight τ through the finite wire, cf. Eq. (9). We provide here first a brief overview of our main results: the finite charging time of the leads imposes two distinct regimes, (i) the large-capacitance regime (see Fig. 2), where the time of flight is much shorter than the charging time, $\tau \ll \tau_{RC}$, and (ii) the more commonly studied complementary small-capacitance regime with $\tau \gg \tau_{RC}$. The latter shows a standard TLL behavior for short times $t \leq \tau$, whereas for long times the finite wire acts as a 0D Fabry-Pérot cavity for the plasmons and free-electron correlations are reobtained (cf. Refs. [3,57,78]). Case (i) shows a richer behavior: at

short times ($t \ll \tau, \tau_{RC}$), the boundary noise inhibits highly excited plasmons and consequently suppresses tunneling, whereas at long times ($t \gg \tau, \tau_{RC}$), both the interactions and noise correlations are averaged out to yield a similar 0D plasmonic Fabry-Pérot behavior. Interestingly, at intermediate times ($\tau < t < \tau_{RC}$), a competition between the TLL correlations and the boundary response ensues, showing both Fabry-Pérot oscillations, as well as nontrivial power laws in the electronic correlations, cf. Eq. (10) and see Fig. 2(a). Furthermore, the power laws show an unexpected dependence on the STM's position [79] that can be observed through [see Fig. 2(b)]

$$\tilde{g}(x, t) \equiv \frac{G^<(x, t)}{G^<(L/2, t)}. \quad (4)$$

In Fig. 3(a), we plot the TDOS in the large-capacitance regime. The spatial dependence can be seen in the intermediate energy regime, see Fig. 3(b). For comparison,

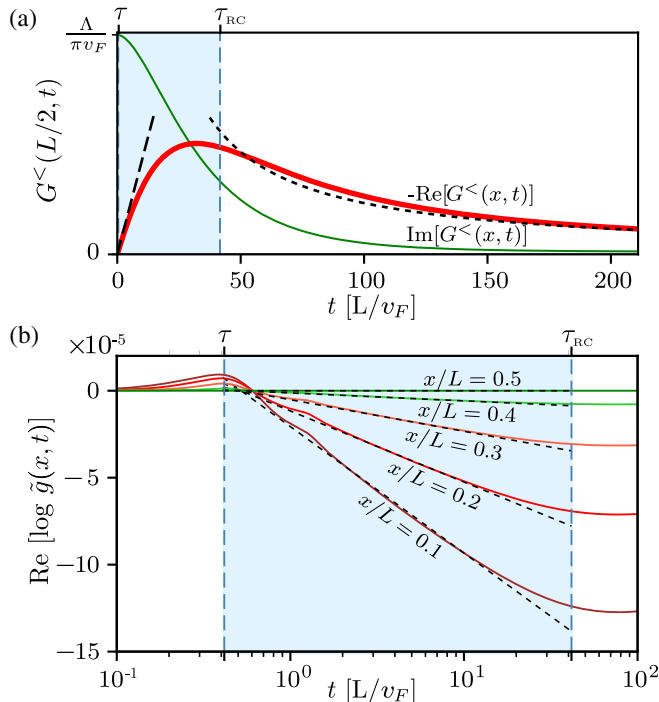


FIG. 2. The Green's function of the wire in the large-capacitance limit. (a) The imaginary (thin green line) and real (thick red line) part of a lesser Green's function $G^<(L/2, t)$ [Eq. (7)]. The dashed lines show the analytically obtained asymptotic limits for long ($t \gg \tau_{RC}$) and short ($t \ll \tau_{RC}$) times. The shaded region (light blue) marks the time interval $\tau < t < \tau_{RC}$ where the interaction-induced correlations in the wire compete with the RC noise. (b) The real part of $\log[\tilde{g}(x, t)]$ [Eq. (4)] exhibiting the nontrivial power-law behavior of the Green's function depending on the position of the STM tip (solid lines). Furthermore, our analytical asymptotic result (dashed lines) [Eq. (11)] agrees with the numerical result (solid lines). In all plots, we use an experimentally realizable interaction parameter $U/v_F = 15$, see, e.g., Refs. [33,34], and large capacitance, $\tau_{RC}/\tau = 100$.

in Fig. 3(c) we plot the TDOS for both finite- and infinite-length interacting wires. The relatively flat peak of the TDOS at low energies is a result of the finite length of the wire that suppresses the ZBA of an infinite TLL [Fig. 3(c)], and is in agreement with the free-electron behavior of the Green's function at long times, cf. Fig. 2(a) and Refs. [57,80]. At high energies, interaction-induced Fabry-Pérot oscillations appear but there is no interaction-dependent power-law growth as compared with both the finite- and infinite-TLL, where the TDOS grows as $\nu(\omega)/\nu_0 \propto \omega^{\alpha-1}$, with $\alpha = (K + K^{-1})/2$ and $\nu_0 = \nu(\omega, \tau_{RC} = 0, K = 1)$ the TDOS into a noninteracting metal with zero capacitance. This is a consequence of a linear, interaction-independent growth of the Green's function at short times, see Fig. 2(a). Hence, the noise of the capacitive leads suppresses the power-law growth and causes the TDOS to drop as $\nu/\nu_0 \propto \omega^{-3}$, in similitude to high-impedance tunnel junctions [1,3].

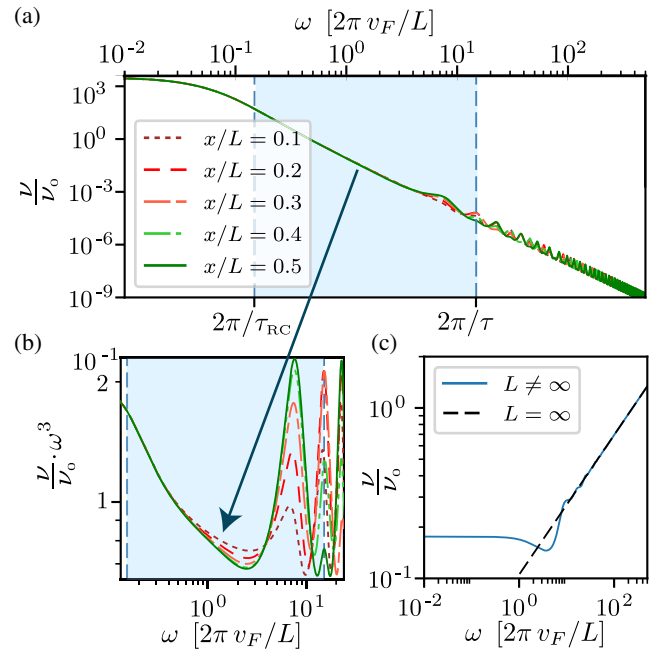


FIG. 3. (a) The normalized TDOS ν/ν_0 in the large-capacitance regime ($\tau_{RC}/\tau = 100$) calculated for five different STM positions in the wire. At high energies, $\omega \gg 2\pi/\tau_{RC}$, the tunneling is suppressed and the TDOS exhibits a power-law decay. Interaction-induced Fabry-Pérot oscillations with a period of $2\pi/\tau$ are present at high energies. For low energies, the TDOS is constant that depends on the value of τ_{RC} . (b) An enlargement on (a) where the TDOS is rescaled by a factor ω^3 such that the difference between different measuring positions inside the wire can be seen more clearly. (c) The TDOS of a finite (blue solid line) and infinite (black dashed line) TLL when the capacitance in the leads is set to zero. In a finite-length TLL, the zero-bias TDOS does not vanish but saturates at a finite value [57]. Note that the normalization of the TDOS is with respect to the value of noninteracting TDOS with vanishing capacitance, ν_0 . The interaction strength used in all plots is $U/v_F = 15$.

Model.—To obtain our results, we closely follow the derivation used in Refs. [57,80]. We consider the Hamiltonian density of a single-channel wire [51,52,54,57,74]

$$\mathcal{H}(x) = -iv_F[\psi_R^\dagger(x)\partial_x\psi_R(x) - \psi_L^\dagger(x)\partial_x\psi_L(x)] + \sum_{\eta,\eta'=L,R} \int dy V_{\eta\eta'}(x-y)\rho_\eta(x)\rho_{\eta'}(y), \quad (5)$$

where the left- and right-moving electrons ($\eta = L, R$) are described by field operators $\psi_\eta(x)$, and $V_{\eta\eta'}(x)$ is the electronic interaction between (normal-ordered) density operators $\rho_\eta(x) = :\psi_\eta^\dagger(x)\psi_\eta(x):$. The first term describes the kinetic contribution for a linearized dispersion $E(\delta k) = v_F\delta k$ around the Fermi momentum k_F , such that the electron field $\psi(x) \simeq e^{-ik_F x}\psi_L(x) + e^{ik_F x}\psi_R(x)$. We further assume that the effective electron-electron interaction is pointlike, i.e., $V_{\eta\eta'}(x) = U\delta(x)$. Note that the linearized dispersion is associated with a bandwidth Λ serving as a high-energy cutoff. Using bosonization [74], we introduce new bosonic field operators $\phi_\eta(x)$ related to the electron density by $\rho_\eta(x) = \partial_x\phi_\eta/2\pi$, with commutation relations $[\phi_{L/R}(x), \partial_x\phi_{L/R}(y)] = \pm 2\pi i\delta(x-y)$. These fields are defined via $\psi_\eta(x) =: \hat{F}_\eta(\Lambda/[2v_F\pi])^{1/2}e^{-i\phi_\eta(x)}$, where the Klein factors \hat{F}_η ensure fermionic anticommutation of ψ_η . In this language, the Hamiltonian takes a simple quadratic form [51,52,74]

$$\mathcal{H}(x) = \left(\frac{v_F}{4\pi} + \frac{U}{8\pi^2}\right) \sum_{\eta=L,R} (\partial_x\phi_\eta)^2 + \frac{U}{4\pi^2} \partial_x\phi_L\partial_x\phi_R. \quad (6)$$

Substituting the bosonization identities into the lesser Green's function of a finite wire, we obtain

$$G_\eta^<(x, t) = \frac{i\Lambda}{2\pi v_F} \exp\left(-\frac{1}{2}\langle[\phi_\eta(x, t) - \phi_\eta(x, 0)]^2\rangle\right), \quad (7)$$

where we have used the fact that the charge fluctuations at the boundaries are Gaussian distributed, and that $\langle F_\eta^\dagger F_\eta \rangle = 1$. Note that the overall Green's function is $G^<(x, t) = G_L^<(x, t) + G_R^<(x, t)$ [72]. Using the equations of motion for the fields ϕ_η [80], we find (in similitude to Ref. [57]) that $G_\eta^<(x, t) \equiv i\Lambda/(2\pi v_F) \exp[-\mathcal{I}(x, t)]$ with the integral

$$\mathcal{I}(x, t) = \int_{-\Lambda}^{\Lambda} \frac{d\omega}{\omega^2} (1 - e^{-i\omega t}) \mathcal{F}(x, \omega) S(\omega), \quad (8)$$

where $S(\omega)$ is as in Eq. (3). The structure function

$$\mathcal{F}(x, \omega) \equiv \frac{1 + \chi - 2\chi \cos(\tau\omega) \cos[2\tau\omega(\frac{1}{2} - \frac{x}{L})]}{1 - \chi \cos(2\tau\omega)} \quad (9)$$

captures both interaction effects through the parameter $\chi^{-1} \equiv [1 + 8\pi v_F/U + 8\pi^2(v_F/U)^2] = [1 - 8K^2/(1 + 6K^2 + K^4)]^{-1}$, and the finite length of the wire through the time of flight of the plasmonic excitations $\tau = (L/v_F)(1 + \pi^{-1}U/v_F)^{-1/2}$. This structure function is equivalent to that of a plasmonic Fabry-Pérot interferometer of length L . Indeed, the same expression is obtained when describing a free particle that is injected at a position x and is reflected from the two boundaries with reflection and tunneling coefficients $r_{A,B} \equiv r$, $t_{A,B} \equiv t$, respectively, where $\chi = 2r^2(1 + r^4)^{-1}$ [cf. Fig. 1(c) and Refs. [20,53,57,87]]. This implies that the plasmonic character of excitations in the wire (due to interactions) causes reflections from the free-electron boundaries.

We can now (i) evaluate $G_\eta^<(x, t)$ numerically using Eqs. (3) and (7)–(9) for different devices with varying τ_{RC}/τ and U/v_F [80], as well as (ii) find analytical asymptotic results for the specific time windows mentioned above. In the latter, we assume that the STM is placed in proximity to the middle of the wire, such that $(1/2 - x/L) \ll 1$.

Large-capacitance regime ($\tau \ll \tau_{RC}$).—For short times, $t \ll \tau \ll \tau_{RC}$, the real-part of the Green's function is linear, while its imaginary part reaches a finite value, i.e., $G^<(x, t \rightarrow 0) = \Lambda(\pi v_F)^{-1}(i - \pi t/2\tau_{RC})$, see Fig. 2(a). This behavior leads to the reduced TDOS at high energies, see Eq. (1) and Fig. 3(a). The large capacitance in the leads effectively acts as a low-pass filter for the plasmonic modes, and inhibits the conversion of high-energy STM electrons into plasmons.

At intermediate times, $\tau \ll t \ll \tau_{RC}$, the main weight of the integral $\mathcal{I}(x, t)$ [Eq. (8)] lies at $\omega \gg \tau_{RC}^{-1}$, where the spectral function is approximated as $S(\omega) \approx 1/\tau_{RC}^2 \omega^{-1}$. We expand the cosine terms in Eq. (9) in small $\tau/t \ll 1$, to obtain

$$G^<(x, t) \approx G^<(L/2, t) \frac{i\Lambda}{2\pi v_F} \frac{1}{(1 + it\Lambda)^{\alpha(x)}}, \quad (10)$$

with a spatially dependent exponent

$$\alpha(x) = \left(\frac{1}{2} - \frac{x}{L}\right)^2 \frac{(K^2 - 1)^2}{2K^3} \frac{\tau^2}{\tau_{RC}^2}. \quad (11)$$

The first factor in Eq. (10) does not depend on the position within the wire. Remarkably, however, the second factor has the same power-law form as that of the Green's function of an infinite TLL, see Eq. (2)—with the notable difference that the exponent has a spatial dependence. This exponent can be extracted from $\tilde{g}(x, t)$ as defined in Eq. (4), see Fig. 2(b).

In the long time limit, $\tau \ll \tau_{RC} \ll t$, the main weight of the integral $\mathcal{I}(x, t)$ [Eq. (8)] stems from small energies, $\omega \ll \tau_{RC}^{-1}$, where the spectral function is approximated as $S(\omega) \approx \omega[1 - f_{FD}(\omega)]$, see Fig. 1(b). Furthermore, for

$\tau \ll t$, the structure function is constant, i.e., $\mathcal{F}(x, \omega) \approx 1 + \mathcal{O}(\tau^2/t^2)$. Hence, the leading term in Eq. (8) becomes $\mathcal{I}(x, t) = \gamma_E + \log(t/\tau_{RC}) + i\pi/2$ with γ_E the Euler constant, resulting in a free-electron response, $G^<(t) = -\Lambda(\pi v_F)^{-1} \exp(\gamma_E)\tau_{RC}/t$ [cf. Eq. (2)]. The plasmons created by the STM reflect back and forth multiple times between the boundaries such that their interference “washes out” the effects of 1D interactions, and a 0D plasmonic cavity forms [3,57].

Conclusion.—The competition between noisy capacitive boundaries and many-body interactions in a finite quantum wire can smoothly alter its temporal and spatial correlations. Specifically, we find that the many-body interactions drive the wire to display a TDOS with features that are dominated by the classical fluctuations of its boundaries. Moreover, the emergent TDOS is predicted to be spatially dependent and can be measured using, e.g., a scanning tunneling microscope. Employing this emergent spatial dependence and control over the classical boundary noise, one can extract the Luttinger parameter of a finite interacting wire with the ability of performing multiple measurements on a single sample. The model considered here is applicable to a broad set of experimental realizations [80]. In the mesoscopic realizations, the leads and STM are available, while in engineered systems they can be designed, e.g., in cold atomic transport experiments, the atomic reservoirs can be embedded into external reservoirs [81] to induce noise and a third reservoir can accomplish the role of an STM. In Ref. [80], we provide a table with realistic parameters for a variety of 1D platforms, demonstrating the experimental feasibility of our model.

We would like to thank B. Rosenow, E. V. Sukhorukov, L. I. Glazman, I. V. Protopopov, I. V. Gornyi, and J. P. Brantut for fruitful discussions. We acknowledge financial support from the Swiss National Science Foundation.

[1] G.-L. Ingold and Y. V. Nazarov, *Charge Tunneling Rates in Ultrasmall Junctions*, edited by H. Grabert and M. H. Devoret (Plenum, New York, 1992).
 [2] T. Ihn, *Electronic Quantum Transport in Mesoscopic Semiconductor Structures* (Springer, New York, 2004).
 [3] G.-L. Ingold and Y. V. Nazarov, arXiv:cond-mat/0508728.
 [4] E. V. Sukhorukov and J. Edwards, *Phys. Rev. B* **78**, 035332 (2008).
 [5] S. Jezouin, M. Albert, F. D. Parmentier, A. Anthore, U. Gennser, A. Cavanna, I. Safi, and F. Pierre, *Nat. Commun.* **4**, 1802 (2013).
 [6] M. Nagae, *Jpn. J. Appl. Phys.* **10**, 1171 (1971).
 [7] B. D. Josephson, *Phys. Lett.* **1**, 251 (1962).
 [8] S. Chakravarty and A. Schmid, *Phys. Rev. B* **33**, 2000 (1986).
 [9] L. P. Kouwenhoven, D. G. Austing, and S. Tarucha, *Rep. Prog. Phys.* **64**, 701 (2001).

[10] D. Goldhaber-Gordon, H. Shtrikman, D. Mahalu, D. Abusch-Magder, U. Meirav, and M. Kastner, *Nature (London)* **391**, 156 (1998).
 [11] L. P. Kouwenhoven and L. Glazman, *Phys. World* **14**, 33 (2001).
 [12] C. Rössler, D. Oehri, O. Zilberberg, G. Blatter, M. Karalic, J. Pijnenburg, A. Hofmann, T. Ihn, K. Ensslin, C. Reichl, and W. Wegscheider, *Phys. Rev. Lett.* **115**, 166603 (2015).
 [13] A. F. Andreev, *Sov. Phys. JETP* **19**, 1228 (1964).
 [14] D. J. van Woerkom, A. Proutski, B. van Heck, D. Bouman, J. I. Väyrynen, L. I. Glazman, P. Krogstrup, J. Nygård, L. P. Kouwenhoven, and A. Geresdi, *Nat. Phys.* **13**, 876 (2017).
 [15] H. J. Suominen, M. Kjaergaard, A. R. Hamilton, J. Shabani, C. J. Palmstrøm, C. M. Marcus, and F. Nichele, *Phys. Rev. Lett.* **119**, 176805 (2017).
 [16] A. Das, Y. Ronen, Y. Most, Y. Oreg, M. Heiblum, and H. Shtrikman, *Nat. Phys.* **8**, 887 (2012).
 [17] S. Tomonaga, *Prog. Theor. Phys.* **5**, 544 (1950).
 [18] J. M. Luttinger, *J. Math. Phys. (N.Y.)* **4**, 1154 (1963).
 [19] F. D. M. Haldane, *J. Phys. C* **14**, 2585 (1981).
 [20] I. Safi and H. J. Schulz, *Phys. Rev. B* **52**, R17040 (1995).
 [21] B. Rosenow, I. P. Levkivskiy, and B. I. Halperin, *Phys. Rev. Lett.* **116**, 156802 (2016).
 [22] O. M. Auslaender, H. Steinberg, A. Yacoby, Y. Tserkovnyak, B. I. Halperin, K. W. Baldwin, L. N. Pfeiffer, and K. W. West, *Science* **308**, 88 (2005).
 [23] Y. Jompol, C. J. B. Ford, J. P. Griffiths, I. Farrer, G. A. C. Jones, D. Anderson, D. A. Ritchie, T. W. Silk, and A. J. Schofield, *Science* **325**, 597 (2009).
 [24] C. L. Kane and M. P. A. Fisher, *Phys. Rev. Lett.* **68**, 1220 (1992).
 [25] K. A. Matveev and L. I. Glazman, *Phys. Rev. Lett.* **70**, 990 (1993).
 [26] E. G. Mishchenko, A. V. Andreev, and L. I. Glazman, *Phys. Rev. Lett.* **87**, 246801 (2001).
 [27] D. B. Gutman, Y. Gefen, and A. D. Mirlin, *Phys. Rev. Lett.* **101**, 126802 (2008).
 [28] W. Apel and T. M. Rice, *Phys. Rev. B* **26**, 7063 (1982).
 [29] T. Giamarchi and H. J. Schulz, *Phys. Rev. B* **37**, 325 (1988).
 [30] J. Vidal, D. Mouhanna, and T. Giamarchi, *Int. J. Mod. Phys. B* **15**, 1329 (2001).
 [31] A. Altland, Y. Gefen, and B. Rosenow, *Phys. Rev. Lett.* **108**, 136401 (2012).
 [32] A. Altland, Y. Gefen, and B. Rosenow, *Phys. Rev. B* **92**, 085124 (2015).
 [33] M. Bockrath, D. H. Cobden, J. Lu, A. G. Rinzler, R. E. Smalley, L. Balents, and P. L. McEuen, *Nature (London)* **397**, 598 (1999).
 [34] Z. Yao, H. W. Ch. Postma, L. Balents, and C. Dekker, *Nature (London)* **402**, 273 (1999).
 [35] J. Cao, Q. Wang, and H. Dai, *Nat. Mater.* **4**, 745 (2005).
 [36] V. V. Deshpande, B. Chandra, R. Caldwell, D. S. Novikov, J. Hone, and M. Bockrath, *Science* **323**, 106 (2009).
 [37] E. Levy, A. Tsukernik, M. Karpovski, A. Palevski, B. Dwir, E. Pelucchi, A. Rudra, E. Kapon, and Y. Oreg, *Phys. Rev. Lett.* **97**, 196802 (2006).
 [38] E. Levy, I. Sternfeld, M. Eshkol, M. Karpovski, B. Dwir, A. Rudra, E. Kapon, Y. Oreg, and A. Palevski, *Phys. Rev. B* **85**, 045315 (2012).

- [39] X. G. Wen, *Phys. Rev. B* **41**, 12838 (1990).
- [40] A. M. Chang, *Rev. Mod. Phys.* **75**, 1449 (2003).
- [41] Y. Ji, Y. C. Chung, D. Sprinzak, M. Heiblum, D. Mahalu, and H. Shtrikman, *Nature (London)* **422**, 415 (2003).
- [42] E. Chow, P. Delsing, and D. B. Haviland, *Phys. Rev. Lett.* **81**, 204 (1998).
- [43] K. Cedergren, R. Ackroyd, S. Kafanov, N. Vogt, A. Shnirman, and T. Duty, *Phys. Rev. Lett.* **119**, 167701 (2017).
- [44] B. Yang, Y.-Y. Chen, Y.-G. Zheng, H. Sun, H.-N. Dai, X.-W. Guan, Z.-S. Yuan, and J.-W. Pan, *Phys. Rev. Lett.* **119**, 165701 (2017).
- [45] T. L. Yang, P. Grišins, Y. T. Chang, Z. H. Zhao, C. Y. Shih, T. Giamarchi, and R. G. Hulet, *Phys. Rev. Lett.* **121**, 103001 (2018).
- [46] S. Krinner, D. Stadler, D. Husmann, J. Brantut, and T. Esslinger, *Nature (London)* **517**, 64 (2015).
- [47] C. Blumenstein, J. Schäfer, S. Mietke, S. Meyer, A. Dollinger, M. Lochner, X. Y. Cui, L. Patthey, R. Matzdorf, and R. Claessen, *Nat. Phys.* **7**, 776 (2011).
- [48] J. Hager, R. Matzdorf, J. He, R. Jin, D. Mandrus, M. A. Cazalilla, and E. W. Plummer, *Phys. Rev. Lett.* **95**, 186402 (2005).
- [49] F. Wang, J. V. Alvarez, S.-K. Mo, J. W. Allen, G.-H. Gweon, J. He, R. Jin, D. Mandrus, and H. Höchst, *Phys. Rev. Lett.* **96**, 196403 (2006).
- [50] T. Podlich, M. Klinke, B. Nansseu, M. Waelsch, R. Bienert, J. He, R. Jin, D. Mandrus, and R. Matzdorf, *J. Phys. Condens. Matter* **25**, 014008 (2013).
- [51] T. Giamarchi, *Quantum Physics in One Dimension* (Clarendon Press, Oxford, 2003).
- [52] I. Levkivskyi, *Mesoscopic Quantum Hall Effect* (Springer-Verlag, Berlin Heidelberg, 2012).
- [53] D. B. Gutman, Y. Gefen, and A. D. Mirlin, *Phys. Rev. B* **80**, 045106 (2009).
- [54] D. B. Gutman, Y. Gefen, and A. D. Mirlin, *Phys. Rev. B* **81**, 085436 (2010).
- [55] S. Eggert, H. Johannesson, and A. Mattsson, *Phys. Rev. Lett.* **76**, 1505 (1996).
- [56] I. Schneider, A. Struck, M. Bortz, and S. Eggert, *Phys. Rev. Lett.* **101**, 206401 (2008).
- [57] Y. V. Nazarov, A. A. Odintsov, and D. V. Averin, *Europhys. Lett.* **37**, 213 (1997).
- [58] A. O. Slobodeniuk, I. P. Levkivskyi, and E. V. Sukhorukov, *Phys. Rev. B* **88**, 165307 (2013).
- [59] D. L. Maslov and M. Stone, *Phys. Rev. B* **52**, R5539 (1995).
- [60] V. V. Ponomarenko, *Phys. Rev. B* **52**, R8666 (1995).
- [61] C. L. Kane and M. P. A. Fisher, *Phys. Rev. B* **46**, 15233 (1992).
- [62] K. A. Matveev, A. V. Andreev, and M. Pustilnik, *Phys. Rev. Lett.* **105**, 046401 (2010).
- [63] S. Tarucha, T. Honda, and T. Saku, *Solid State Commun.* **94**, 413 (1995).
- [64] H. Pothier, S. Guéron, N. O. Birge, D. Esteve, and M. H. Devoret, *Phys. Rev. Lett.* **79**, 3490 (1997).
- [65] A. Anthore, F. Pierre, H. Pothier, and D. Esteve, *Phys. Rev. Lett.* **90**, 076806 (2003).
- [66] A. Luther and I. Peschel, *Phys. Rev. B* **9**, 2911 (1974).
- [67] M. P. A. Fisher and L. I. Glazman, Transport in a one-dimensional Luttinger liquid, in *Mesoscopic Electron Transport*, edited by L. L. Sohn, L. P. Kouwenhoven, and G. Schön (Springer, Netherlands, 1997), pp. 331–373.
- [68] I. Safi and H. J. Schulz, *Phys. Rev. B* **59**, 3040 (1999).
- [69] S. Eggert, *Phys. Rev. Lett.* **84**, 4413 (2000).
- [70] C. S. Peça, L. Balents, and K. J. Wiese, *Phys. Rev. B* **68**, 205423 (2003).
- [71] M. Fabrizio and A. O. Gogolin, *Phys. Rev. B* **51**, 17827 (1995).
- [72] H. Bruus and K. Flensberg, *Many-Body Quantum Theory in Condensed Matter Physics: An Introduction* (Oxford University, Oxford, 2004).
- [73] E. M. Lifshitz and L. P. Pitaevskii, *Statistical Physics, Part 2, Landau and Lifshitz Course of Theoretical Physics Vol. 9* (Butterworth/Heinemann, Oxford, 1980).
- [74] J. von Delft and H. Schoeller, *Ann. Phys. (Berlin)* **7**, 225 (1998).
- [75] S. Machlup, *J. Appl. Phys.* **25**, 341 (1954).
- [76] A. Carmi and Y. Oreg, *Phys. Rev. B* **85**, 045325 (2012).
- [77] E. Shahmoon and U. Leonhardt, *Sci. Adv.* **4**, eaaq0842 (2018).
- [78] S. Pugnetti, F. Dolcini, D. Bercioux, and H. Grabert, *Phys. Rev. B* **79**, 035121 (2009).
- [79] The spatial dependence we discuss in this Letter is different than that of a wire with open boundaries [Ref. [55]].
- [80] See Supplemental Material at <http://link.aps.org/supplemental/10.1103/PhysRevLett.122.126802> for additional details on: (1) equations of motion for bosonic fields, (2) analytical results for the Green's function in different time regimes, (3) numerical results for the Green's function and the TDOS in different devices, and (4) a table with realistic parameters for a variety of 1D platforms, which includes Refs. [33,34,38,47,49,50,57,81–86].
- [81] S. Uchino, M. Ueda, and J.-P. Brantut, *Phys. Rev. A* **98**, 063619 (2018).
- [82] E. G. Idrisov, I. P. Levkivskyi, and E. V. Sukhorukov, *Phys. Rev. B* **96**, 155408 (2017).
- [83] S. J. Tans, A. R. M. Verschueren, and C. Dekker, *Nature (London)* **393**, 49 (1998).
- [84] G. Pagano, M. Mancini, G. Cappellini, P. Lombardi, F. Schäfer, H. Hu, X.-J. Liu, J. Catani, C. Sias, M. Inguscio, and L. Fallani, *Nat. Phys.* **10**, 198 (2014).
- [85] M. Lebrat, P. Grišins, D. Husmann, S. Häusler, L. Corman, T. Giamarchi, J.-P. Brantut, and T. Esslinger, *Phys. Rev. X* **8**, 011053 (2018).
- [86] I. Gradshteyn and I. S. Ryzhik, *Table of Integrals, Series, and Products*, 8th ed. (Academic Press, New York, 2004).
- [87] In Refs. [20,53,57], the interaction-dependent scattering amplitudes at the boundary of the wire that enter Eq. (9) were derived microscopically. Our results correspond to the sharp boundary limit of Ref. [53] where the reflection coefficient is $r = (1 - K)/(1 + K)$.